VILNIUS UNIVERSITY

Giedrius
STABINGIS

Statistical decisions for spatial information in digital images

SUMMARY OF DOCTORAL DISSERTATION

Natural Sciences,
Informatics N 009

VILNIUS 2019

This dissertation was written between 2014 and 2018 at Vilnius University.

Academic supervisor:
Prof. Habil. Dr. Gintautas Dzemyda (Vilnius University, Natural Sciences, Informatics – N 009).
Academic consultant:
Prof. Dr. Kęstutis Dučinskas (Klaipėda University, Natural Sciences, Informatics – N 009).

This doctoral dissertation will be defended at the public meeting of the Dissertation Defence Panel:

Chairman:
Prof. Dr. Romas Baronas (Vilnius University, Natural Sciences, Informatics – N 009).

Members:
Prof. Habil. Dr. Romualdas Baušys (Vilnius Gediminas Technical University, Technology Sciences, Informatics Engineering – T 007),
Prof. Dr. Vacius Jusas (Kaunas University of Technology, Natural Sciences, Informatics – N 009),
Prof. Dr. Audris Mockus (University of Tennessee, USA, Natural Sciences, Informatics – N 009),
Prof. Dr. Dalius Navakauskas (Vilnius Gediminas Technical University, Technology Sciences, Informatics Engineering – T 007).

The dissertation will be defended at the public meeting of the Dissertation Defence Panel at 12:00 a. m. on the 27th of June, 2019 in the auditorium 203 of the Institute of Data Science and Digital Technologies of Vilnius University.
Address: Akademijos street 4, LT-04812 Vilnius, Lithuania.
The summary of the doctoral dissertation was distributed on the 27th of May, 2019.
The text of this dissertation can be accessed at the library of Vilnius University, as well as on the website of Vilnius University: www.vu.lt/lt/naujienos/ivykiu-kalendorius

VILNIAUS UNIVERSITETAS

Giedrius
STABINGIS

Statistiniai sprendimai erdvinei informacijai skaitmeniniuose vaizduose

DAKTARO DISERTACIJOS SANTRAUKA

Gamtos mokslai,
informatika N 009

VILNIUS 2019

Disertacija rengta 2014-2018 metais Vilniaus universitete.

Mokslinis vadovas:
prof. habil. dr. Gintautas Dzemyda **(**Vilniaus universitetas, gamtos mokslai, informatika – N 009).

Mokslinis konsultantas:
prof. dr. Kęstutis Dučinskas (Klaipėdos universitetas, gamtos mokslai, informatika – N 009).

Gynimo taryba:
Pirmininkas:
prof. dr. Romas Baronas (Vilniaus universitetas, gamtos mokslai, informatika – N 009).

Nariai:
prof. habil. dr. Romualdas Baušys (Vilniaus Gedimino technikos universitetas, technologijos mokslai, informatikos inžinerija – T 007),
prof. dr. Vacius Jusas (Kauno technologijos universitetas, gamtos mokslai, informatika – N 009),
prof. dr. Audris Mockus (Tenesio universitetas, JAV, gamtos mokslai, informatika – N 009),
prof. dr. Dalius Navakauskas (Vilniaus Gedimino technikos universitetas, technologijos mokslai, informatikos inžinerija – T 007).

Disertacija ginama viešame Gynimo tarybos posėdyje 2019 m. birželio mėn. 27 d. 12 val. Vilniaus universiteto Duomenų mokslo ir skaitmeninių technologijų instituto 203 auditorijoje.
Adresas: Akademijos g. 4, LT-08412 Vilnius, Lietuva.
Disertacijos santrauka išsiuntinėta 2019 m. gegužės 27 d.
Disertaciją galima peržiūrėti Vilniaus universiteto bibliotekoje ir Vilniaus universiteto interneto svetainėje adresu: https://www.vu.lt/naujienos/ivykiu-kalendorius

1. INTRODUCTION

1.1. Research area

The main goal of image analysis is to acquire knowledge from images needed for the subject area in order to make a decision. Spatial information describes the connection between the spatial data and the features of this data. Image analysis objects for which spatial information is available are whole images, areas of the images and their sets, and separate image pixels. Spatial information and its applications are analyzed and applied in this dissertation for objects in images and in their sets (images in 3D space). Separate pixels and their sets are considered. Such objects are described not only by their location in space, but also the relationship between these objects: spatial distance, spatial dependence – spatial autocorrelation, information of class labels and other statistical information linked with these objects. The usage of information from objects in images in order to acquire new information is also considered. In this case image size or the size of the main object in the image is used in order to achieve methods' universality.

1.2. Relevance of the Problem

Data collection in the form of digital images is inseparable in many fields of our day life. Images are gathered and archived in almost every field. Because of the improvement of the technical equipment, images, image retrieval, collection, and analysis have become an integral part of biomedical, natural and social sciences, and engineering. Image analysis is already becoming an important new tool and information retrieval for image extraction equipment. This area is facing new challenges and opportunities.

The use of spatial information in a study of image classification began a long time ago (Haralick, 1979), and the advance of the technical possibilities in the data analysis of the relevance of these studies is growing (Wang et al., 2016). In practice, the image analysis and processing are used in the range of methods that were created a long time ago and are now used for many issues. However, these methods are studied and perfected even today (Wang et al., 2016; Miri

et al., 2017; Troya-Galvis et al., 2018). Much attention is paid to image filtering (Mun et al., 2018; Guo et al., 2018), object extraction, segmentation, recognition, classification (Öztürk et al., 2018), (Krishnan et al., 2018) and other methods.

One of the problems in image classification is to divide the observed image into several regions by labeling its pixels. This is done by taking into account point features and information about their spatial relationships with the training sample. Author Switzer was the first who used spatial relationships in classification (Switzer, 1980). Geostatistical methods are widely used in image classification. These methods use spatial autocorrelation, which shows the degree to which the correlation changes with the distance between objects (Liu et al., 2009) and it is being studied in the methods proposed by many authors (see Atkinson et al., 2009; Comber 2013; Li et al., 2014). Spatial autocorrelation is used in Bayes discriminant functions, where the parameters are often evaluated considering that the object used for classification is independent from training sample objects. In the article (Dučinskas, 2009) the parameters were evaluated taking into account the spatial dependence with the training sample. The applications of Bayes discriminant functions in image analysis and the influence of spatial correlation were analyzed in the dissertation (Stabingienė, 2012).

Eye fundus vessels are the only human blood vessels that can be observed by non-invasive imaging techniques (Miri et al., 2017; Fraz et al., 2014). Manual and automated structural analysis is often applied to eye fundus images (Mirsharifa et al., 2013; Sim et al., 2015). This analysis makes it easier to diagnose diseases, especially in the early stages of the disease (Li et al., 2014). Many diseases can be early diagnosed from eye fundus image analysis according to several different signs. Ophthalmologists associate certain features according to arterial and vein widths with some diseases such as diabetic retinopathy, atherosclerosis, hypertension, and so on. The diseases affect arteries and veins, resulting in an abnormal artery and vein width ratio.

When new technical possibilities emerged, the methods of deep learning were researched and applied (LeCun et al., 2015). Convolutional neural networks are widely used in image analysis (Krizhevsky et al., 2012), which help to solve very complex problems.

The 3D convolutional neural network is used to identify human actions from video (Ji et al., 2013). Adaptive gesture recognition system is published in the article (Neverova et al., 2016). Human face analysis possibilities in DeepFace system are presented in (Taigman et al., 2014). The methods themselves are also being studied (Yosinski et al., 2014). The analysis of the eye fundus image is not an exception either; here these methods are applied in various situations (Almotiri et al., 2018). The convolutional neural networks use information extracted from digital images about objects in them using a variety of filters that are widely used in image processing. The lack of information required for such methods is solved through image augmentation techniques, which also employ a variety of image analysis techniques. These examples illustrate the fact that knowledge of patterns in digital images can be used to improve the existing or new approaches in deep learning and in other fields.

1.3. The Aim and Tasks of the Research

The goal of the research is to find new statistical decisions for spatial information in digital images, to apply and investigate their application possibilities for analyzing eye fundus images.

The object of the research is the spatial information in digital images.

To realize the aim of research, it is necessary to solve the following tasks:

1. To analyze the influence of spatial correlation to supervised classification methods.
2. To insert the influence of spatial correlation into prior probabilities of plug-in Bayes discriminant functions.
3. To propose new neighborhood selection methods and to investigate their influence on classification; to find the best neighborhood selection method for classification of image places further from the training sample.
4. To examine statistical image analysis methods employed for eye fundus images used in eye fundus vessels research.
5. To find the way of using statistical decisions for spatial information in eye fundus blood vessel measurements.

6. To use spatial information in eye fundus blood vessel classification for problem solving.

1.4. Scientific Novelty

1. Classification method SCRD is developed; class prior probabilities depend on the training sample in this method taking into account spatial correlation.
2. The influence of neighborhood selection methods on supervised classification is analyzed, and the best technique for the SCRD method is determined.
3. SCRD classification method based on spatial distance and correlation is generalized for data with 3D coordinate systems.
4. Adaptive eye fundus image analysis method is developed.
5. Spatial distance-based function is used for blood vessel profile information extraction applied in blood vessel width measurements in eye fundus images.
6. Automatic classification method, based on spatial normalization of the features, is developed. The method is used for artery-vein ratio calculations.

1.5. Statements to be Defended

1. Prior class probabilities depend on spatial correlation between the training sample and object to be classified.
2. The choice of the neighborhood selection method makes more precise classification for image places where the training sample for one of the classes is not available.
3. The usage of spatial functions in image profile extraction lets us use the general measurement method for eye fundus images of different sizes.
4. Spatial distance employed in normalization of features used in classification helps to reduce the influence of uneven image lightening.

1.6. Approbation of the Research

The results of the research were published in two peer-reviewed journals, in five peer-reviewed conference proceedings journals and were presented and discussed at eleven national and international conferences.

1.7. Outline of the Dissertation

The dissertation consists of five chapters and references. The chapters of the dissertation are as follows: Introduction; Spatial information and image analysis; Spatial classification rule; Eye fundus blood vessel classification; and Conclusions. The dissertation also includes a list of notation and abbreviations. The scope of the work is 110 pages that include 36 figures and 10 tables. The list of references consists of 125 sources.

2. SPATIAL INFORMATION AND IMAGE ANALYSIS

In this chapter spatial information used in image analysis is considered. Methods for extracting information from images are analyzed. These methods are used for image filtering, object extraction, recognition and classification. Geostatistical, image processing, deep learning and other methods are analyzed. Eye fundus image analysis is studied as a field of applications.

Spatial data is any knowledge of location, forms, relationships between them, and geographical features. The main feature of spatial data is the relation of data to the coordinate system. In geography or geostatistics, spatial data are defined as data directly or indirectly associated with a particular location or geographical area (Cressie, 1993). In digital images, spatial data is associated with image coordinates or image regions.

The 2D digital image consists of a pixel grid. The pixel is the smallest image element. Each pixel corresponds to one or more values called point intensity values. The intensity values differ depending on the location of the point $s(x, y)$, where x corresponds to the horizontal position of the pixel and y is the vertical position. Image $I(s)$ is a function that links image coordinates (point) with intensity values. For

color image encoded by *RGB* (Red, Green, Blue) color mixing, $I(s) = \big(I_R(s), I_G(s), I_B(s)\big)$. Since the points in digital images are at equal distances in the $\mathbb{R}^2$ space, the pixel matrix corresponds to the values of the image function $I(s)$ at those points. In digital images, coordinates and corresponding intensity values are treated as spatial data.

Spatial information defines the physical meaning of objects and the relationship between objects. In geostatistics spatial information is a link between locations, people, activities, and other objects. In image analysis spatial information links pixels or areas of pixels form spatial data. Spatial information in digital images is characterized by clusters, textures, distances, correlations, classes and other. This information derives from spatial data and is further used to generate knowledge and make decisions as shown in Fig. 1.

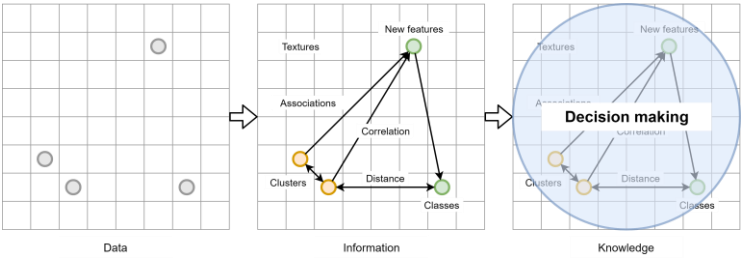

Fig. 1. Data, information and knowledge in image analysis.

Formally, we can define spatial data as a result of spatial observations. When observation is performed at the d-dimensional Euclidean space point $s \in \mathbb{R}^d$, the observation at $Z(s)$ space point s is variate. Then the mathematical model of spatial data (spatial population) is a random field (RF) $\{Z(s): s \in D\}$, where $D \subset R^d$ is a set of spatial indexes, and the realization of a random field is marked as $\{z(s): s \in D\}$.

Supervised classification methods are often considered to be independent from the training sample points. In addition to the assumption of independence, the methods can use not only training sample data, but also spatial information from this data. The use of this information improves the way the methods work and allows the

model to include spatial autocorrelation and other information into the model.

It has been found that spatial correlation in classification is without the classification point independence from the training sample assumption, so spatial distance information of the training sample is used for more accurate classification. It is also useful to identify other ways of taking into account the influence of spatial dependence on classification. This can be done by calculating the prior class probabilities.

The analyzed Bayes discriminant functions with spatial dependence provide high accuracy. Modern technologies also produce 3D images. These images are often used in medicine (CT, MRT). Therefore, it is useful to generalize spatially-based methods so that they can be applied to images of a higher spatial dimension.

Currently, the deep learning methods are in focus. In image analysis, especially in the area of image classification, convolutional neural networks are investigated and applied. These, though requiring large computing resources, produce very good results and generate relevant application opportunities. The convolutional neural networks use spatial information from digital images about objects in these images applying filters widely used in image processing. Problems with lack of training information are solved by image augmentation, which also uses a variety of image analysis and processing techniques. These examples illustrate that knowledge of patterns in digital images can become a tool for developing deep learning and other methods.

One of the areas of the application of spatial information in image analysis is the analysis of medical images. This analysis is a useful tool for monitoring disease progression and early diagnosis. One of the important areas of application is the analysis of the eye fundus images. In this area, spatial information-based statistical decisions can be used to create more accurate and adaptive analytical tools.

Several features are used to identify illnesses using eye fundus image analysis. One of these features is the ratio of arteries to veins – *AVR*. Calculating this parameter for an ophthalmologist takes a lot of time, and automated and fully automated systems make it easier to do the calculations and to diagnose the disease.

Calculating *AVR* automatically is a complex task because it consists of several steps. It is important to identify the optic nerve disc

(*OD*), to determine the measuring zone of the *AVR* parameter, to identify the major blood vessels, to classify them into vein and artery classes, and to measure the vascular width. The most difficult parts of this process are the classification of blood vessels and the measurements of vascular width. The main causes of classification errors are uneven lighting, vessel overlapping and noise. These problems must be taken into account when developing automatic methods.

Various filters and other operations are often useful for analyzing eye fundus images. Many of these operations require specific parameters to be chosen. Methods often use image reduction operations to align parameter values. This will result in the loss of image information. Instead of reducing images (by aligning sizes), it is more appropriate to recalculate the parameters that depend on the image size while developing these methods.

Many of the *AVR* measurement methods use the LDA classification adjusted with a certain image base. However, when creating an automatic method of calculating *AVR* with images from an unknown image database, the classification method should be independent of it.

3. SPATIAL CLASSIFICATION RULE

In this chapter, the statistical supervised classification method is presented and analyzed. Spatial classification rule based on the plug-in Bayes discriminant function with posterior distribution of class label ignoring the distances among the locations is denoted by SCR. The extended method depending on distances among unclassified locations and training sample locations is called SCRD (Spatial Classification Rule with Distance).

3.1. Method description

For the proposed method features are modeled by stationary Gaussian random field (GRF) $\{Z(s): s \in D \subset \mathbb{R}^2\}$, and class labels are modeled by discrete Markov random field (MRF). Such modeling is common in image analysis. In the context of image analysis index s means pixel.

The marginal model of observation *Z(s)* in class Ω_l is $Z(s) = \mu_l + \varepsilon(s)$, where μ_l is the mean, and the error term $\varepsilon(s)$ is generated by zero-mean stationary Gaussian random field $\{\varepsilon(s): s \in D\}$ with covariance function defined by model $cov\{\varepsilon(s), \varepsilon(u)\} = \sigma^2 r(s-u)$ for all $s, u \in D$, where *r(s - u) = r(h)* is the spatial correlation function and σ^2 is variance as a scale parameter. During the experiments, the exponential covariance function is used:

$$C(h) = \sigma^2 \cdot e^{-\frac{h}{\alpha}} \quad (1)$$

where α is the correlation range parameter.

$$r(s-u) = r(h) = e^{-\frac{h}{\alpha}} \quad (2)$$

where *h* is the Euclidean distance between *s* and *u* locations.

Let $L = \{1,2\}$ be a label set. A label of pixel $s \in D$ associated with $Z(s)$ is a random variable $Y(s)$ taking values in L. Let $S_n = \{s_i \in D; i = 1, \dots, n$ be a set of training pixels. Set $Y = (Y(s_1), \dots, Y(s_n))'$ and $Z = (Z(s_1), \dots, Z(s_n))'$ and call them labels vector and features vector respectively. Thus, the vector $T = (Z, Y)$ constitutes the training sample. Suppose that the event $\{T=t\}$ is equivalent to the event $\{Z = z\} \cap \{Y = y\}$, where *t*, *z*; *y* are the realizations of the corresponding random vectors.

Let's assume that the model of *Z* for given $Y = y$ is $Z = X_y\mu + E$, where X_y is a design matrix, $\mu' = (\mu_1, \mu_2)$ and *E* is the *n*-vector of random errors that has multivariate Gaussian distribution $\mathcal{N}_n(0, \sigma^2 R)$. Let's consider the problem of classification (estimation of $Y(s_0)$) of the feature observation $Z_0 = Z(s_0)$, $s_0 \in D$, $s_0 \notin S_n$ with the given training sample $T=t$. Here s_0 is the location of the observation to be classified. $Z_n = (Z(s_i | s_i \in S_n))$ is the feature vector from the neighbor observations of the observation to be classified. Denote by r_0 the vector of spatial correlations between Z_0 and Z_n. Also denote by *R* the matrix of spatial correlations among components of Z_n. *R* and r_0 components are calculated according to the Eq. (2). Since Z_0 is correlated with the training sample, we have to deal with conditional

Gaussian distribution of Z_0 given $T=t$ ($Z=z$, $Y=y$) with means μ_{lt}^0 and variance σ_{0t}^2 that are defined by

$$\mu_{lt}^0 = E(Z_0|T=t; Y(s_0)=l) = \mu_l(s_0) + \alpha_0'(z_0 - X_y\mu),$$
$$\sigma_{0t}^2 = V(Z_0|T=t; Y(s_0)=l) = \sigma^2 R_{0n}, \quad (3)$$

where $\alpha_0' = r_0' R^{-1}$, $R_{0n} = 1 - r_0' R^{-1} r_0$ and $l = 1, 2$.

In this methodology assumption that the posterior distribution of $Y(s_0)$ given $T=t$ depends only on $Y=y$ and N_0 is made. The posterior distribution of $Y(s_0)$ is

$$\pi_l(y) = P(Y(s_0) = l|T=t), l = 1,2. \quad (4)$$

Suppose that means $\{\mu_l(s)\}$ and σ^2 are unknown and need to be estimated from training sample T. Let $\hat{\mu}$ and $\hat{\sigma}^2$ be the estimates of μ and σ^2, based on $T=t$. Let's denote the three component vector of parameters by $\Psi' = (\mu, \sigma^2)$ and the vector of their estimates by $\hat{\Psi}' = \left(\hat{\mu}, \hat{\sigma}^2\right)$.

The plug-in Bayes discriminant function (PBDF) is obtained by replacing the parameters in Bayes discriminant function (BDF) with their estimates based on $T=t$. Then PBDF to the classification problem specified above is

$$W_t\left(Z_0; \hat{\Psi}\right) = \left(Z_0 - \frac{\left(\hat{\mu}_{1t}^0 + \hat{\mu}_{2t}^0\right)}{2}\right)\frac{\left(\hat{\mu}_{1t}^0 - \hat{\mu}_{2t}^0\right)}{\hat{\sigma}_{0t}^2} + \gamma(y), \quad (5)$$

$$\hat{\mu}_{lt}^0 = \hat{\mu}_l + \alpha_0'\left(z_n - X_y\hat{\mu}\right),$$
$$\hat{\mu}_{1t}^0 = E(Z_0|T=t; Y(s_0)=1) = \hat{\mu}_1 + \quad (6)$$
$$\alpha_0'\left(z_n - X_y\begin{pmatrix}\hat{\mu}_1 \\ \hat{\mu}_2\end{pmatrix}\right),$$

$$\hat{\mu}_{2t}^{0} = E(Z_0|T = t; Y(s_0) = 2) = \hat{\mu}_2 + \alpha_0' \left(z_n - X_y \begin{pmatrix} \hat{\mu}_1 \\ \hat{\mu}_2 \end{pmatrix} \right),$$

$$\hat{\mu} = \left(X_y' R^{-1} X_y \right)^{-1} X_y' R^{-1} Z = \begin{pmatrix} \hat{\mu}_1 \\ \hat{\mu}_2 \end{pmatrix},$$

$$\hat{\sigma}_{0t}^2 = Var(Z_0|T = t; Y(s_0) = l) = \hat{\sigma}^2 R_{0n}, \quad \hat{\sigma}^2 = \frac{(Z - X_y\hat{\mu}) R^{-1} (Z - X_y\hat{\mu})}{n-2}, \tag{7}$$

$$\gamma(y) = ln(\pi_1(y)/\pi_2(y)). \tag{8}$$

SCR is denoted as the classification rule based on the posterior distribution of $Y(s_0)$ specified by

$$\pi_1(y) = \frac{1}{1 + e^{\rho\left(1 - \frac{2n_1}{n}\right)}}, n_1 = 0,1, \dots, n, \tag{9}$$

when $I_0 = \{i: s_i \in N_0 = NN(8), i = 1, \dots, n\}$ and where ρ is non-negative constant called a clustering parameter, and n_1 is the number of locations from N_0 with label equal 1. Here $NN(8)$ is the nearest neighbor scheme with eight nearest neighbors.

The proposed spatial classification rule SCRD is based on the following posterior distribution

$$\pi_1(y) = \frac{\sum_{i \in I_0} \frac{\delta(y_i = 1)}{d(s_i, s_0)}}{\sum_{i \in I_0} \sum_{j=1}^{2} \frac{\delta(y_i = j)}{d(s_i, s_0)}} = \frac{\sum_{i \in I_0} \frac{\delta(y_i = 1)}{d(s_i, s_0)}}{\sum_{i \in I_0} \frac{1}{d(s_i, s_0)}}, \tag{10}$$

where $\delta(\cdot)$ is 0 – 1 indicator function and $d(\cdot, \cdot)$ denotes the Euclidean distance function between locations. For the case of two classes $\pi_2 = 1 - \pi_1$.

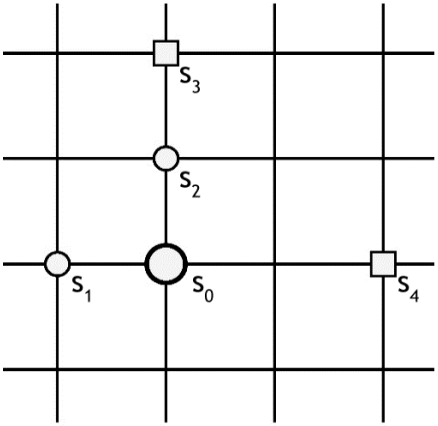

Fig. 2. Illustration of spatial situation.

According to the situation illustrated in Fig. 2, using the SCR method the probabilities of class labels are $\pi_1 = \frac{1}{2}$ and $\pi_2 = \frac{1}{2}$. While using the SCRD method, the prior probability of the first class increases because the observation to be classified s_0 is closer to the s_1 and s_2 locations than to the locations s_3 and s_4. According to the SCRD method for the situation illustrated in Fig. 2 π_1, prior probability is calculated:

$$\pi_1(y) = \frac{\frac{\delta(y_1 = 1)}{1} + \frac{\delta(y_2 = 1)}{1} + \frac{\delta(y_3 = 1)}{2} + \frac{\delta(y_4 = 1)}{2}}{\sum_{i=I_0} \left(\frac{\delta(y_i = 1)}{d(s_i, s_0)} + \frac{\delta(y_i = 2)}{d(s_i, s_0)} \right)} = \tag{11}$$

$$= \frac{2}{\left(\frac{1}{1} + \frac{0}{1}\right) + \left(\frac{1}{1} + \frac{0}{1}\right) + \left(\frac{0}{2} + \frac{1}{2}\right) + \left(\frac{0}{2} + \frac{1}{2}\right)} = \frac{2}{3}.$$

3.2. Method operation study

The aim of this experiment is to test the overall accuracy of the proposed method. The artificially corrupted images of different symbols are used in this experiment for classification. All calculations are done with the statistical computing software R (R Core Team, 2018).

In this experiment 100 different images are used. The dimensions of every image are 200×200 pixels. Every initial image consists of pure white and pure black color pixels. All the images are prepared outside the R software and read using "rtiff" package. This package reads .tiff type image and produces the number matrix corresponding image pixels. With this package black pixels become 0 and white pixels become 1 inside of the number matrix. All other gray level pixels are from the interval (0; 1).

According to every initial image, the training sample is randomly generated for every class; 0.8% of image points are used in the training sample. That is only about 320 from 40 000 points are taken for the training sample. The first class is sampled from white pixels and the second from black pixels. Sampling is done proportionally for each class.

Further initial images are corrupted by spatially correlated Gaussian random fields. Random fields are generated with "geoR" package inside R software using isotropic exponential covariance function and variance equal to 1. During this experiment, the influence of correlation range parameter α is also investigated. Therefore, each of the initial images is corrupted by four different Gaussian random fields where spatial correlation range parameter α is equal to 5, 10, 20 and 50. Four different Gaussian random fields generated with different α parameter values are shown in Fig. 3. These four Gaussian random fields are generated separately for every initial image.

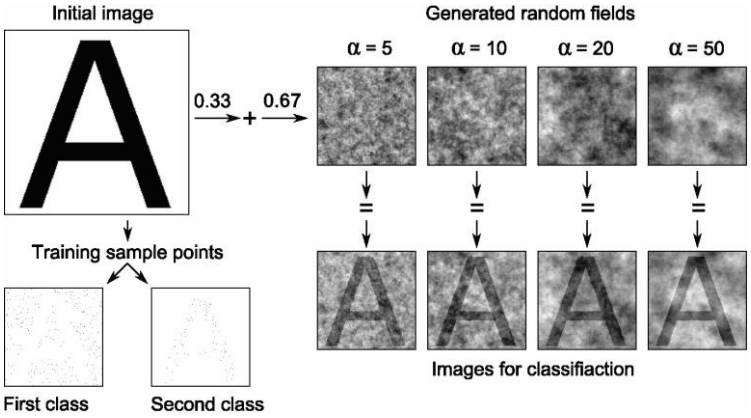

Fig. 3. Experiment preparation scheme: 100 different images for 4 different α values are prepared according to this scheme.

Every generated random field is a number matrix and this matrix is normalized in order to gain values between 0 and 1. Then such field is combined with initial image by summing their matrix values according to the equation:

$$I_\varepsilon = (1 - p_\varepsilon) \cdot I_Z + p_\varepsilon \cdot I_{GRF}, \qquad (12)$$

here $p_\varepsilon \in [0; 1]$ is noise level, I_ε is a new image with spatially correlated noise, I_Z – initial image and I_{GRF} is an image of spatially correlated noise.

During the experiment $p_\varepsilon = 0.67$ value or image and noise proportion 0.33:0.67 was used. This is done in order to get an image, which is corrupted hard enough for such classification problems. The whole experiment preparation scheme is shown in Fig. 3. According to the preparation scheme, 100 different images were prepared for classification. This gives us 400 different images because of four different α values which were investigated.

3.3. Method results

During the experiment all 400 different corrupted images are classified by six different classification methods. The classification

process is done using six different classification methods: SCR, SCRD and other four supervised classification methods that are commonly used for image per pixel classification. These methods are Logit, RF, NNet and SVM. After the classification plenty of resulting images were obtained. One of the classification sets with the letter “B” is presented in Fig. 4.

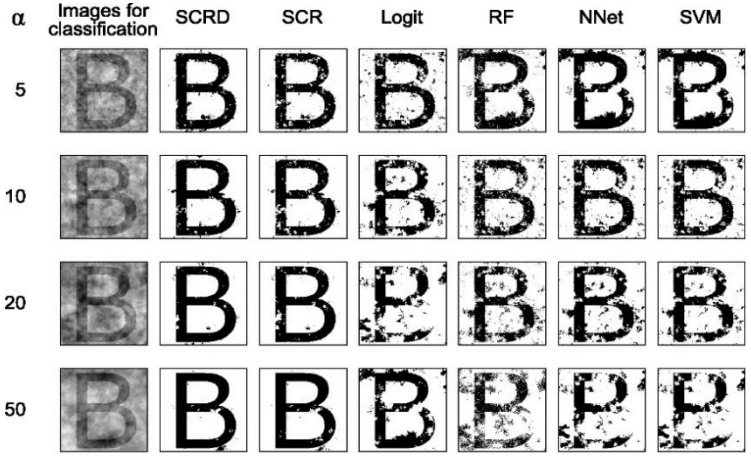

Fig. 4. Visual results of the experiment. Such classification sets are obtained for 100 different initial images.

According to the visual classification results presented in Fig. 4, it can be shown that the SCR method performs better than the other commonly used classification methods. The new classification method SCRD proposed here is even better. The classification errors appear at the same places for both methods but for the new method these error places are smaller. Furthermore, it can be seen from the visual results that they become better for the SCR and SCRD methods when the spatial correlation range parameter α r increases. The other commonly used methods produce opposite results.

After the classification all the resulting images are analyzed numerically. The average classification accuracy, standard deviation of classification accuracy, the minimum and the maximum classification accuracies are calculated for every method and presented in the Table 1.

As it was mentioned before, the influence of the parameter α is tested in this paper. The results of the overall classification accuracy for increasing the α parameter are presented in Table 2.

Table 1. Overall classification accuracy results.

Method	**SCRD**	**SCR**	**Logit**	**RF**	**NNet**	**SVM**
Average	0.984	0.977	0.908	0.888	0.907	0.908
σ	0.009	0.014	0.030	0.037	0.030	0.030
Min	0.946	0.925	0.759	0.731	0.761	0.756
Max	0.999	0.999	0.978	0.965	0.977	0.978

Table 2. Average classification accuracy according to parameter α.

α	**Method**					
	SCRD	**SCR**	**Logit**	**RF**	**NNet**	**SVM**
5	0.973	0.962	0.927	0.910	0.926	0.926
10	0.980	0.971	0.915	0.896	0.914	0.915
20	0.988	0.984	0.905	0.882	0.904	0.904
50	0.994	0.993	0.886	0.863	0.886	0.886

According to the numerical results presented in Tables 1 and 2, it can be stated that the SCRD method is better than the earlier SCR method. The classification accuracy for the SCRD and SCR methods increases for the larger α values while the accuracy of the other commonly used classification methods decreases.

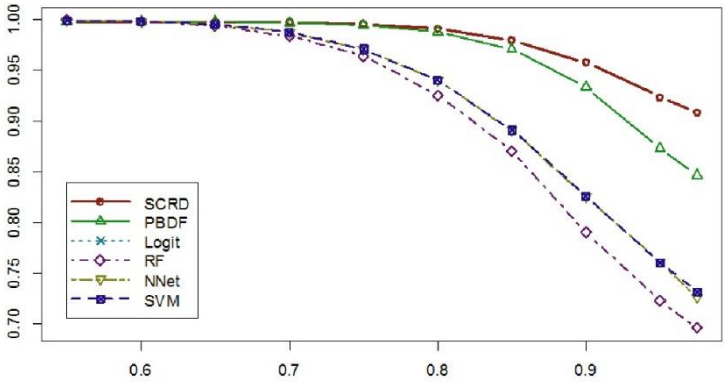

Fig. 5. Overall accuracy results of classification.

The influence of noise level p_ε was tested more deeply in further experimental research. During this experiment it was determined that when noise level $p_\varepsilon \geq 0.75$ the SCR and SCRD methods start to gain advantage over other methods. The SCRD method gets the advantage over the SCR method when $p_\varepsilon \geq 0.85$. The results of this research are presented in Fig. 5.

3.4. Other research of the method

Analyzing the results of the previous experiments more deeply some important cases were noticed. During the classification some parts were misclassified because there were no training samples corresponding to the appropriate class. These parts were surrounded by the training sample points of other class. A few such situations are presented in Fig. 6. This situation is examined by proposing to use different neighborhood schemes, which always include at least one training sample element from each class.

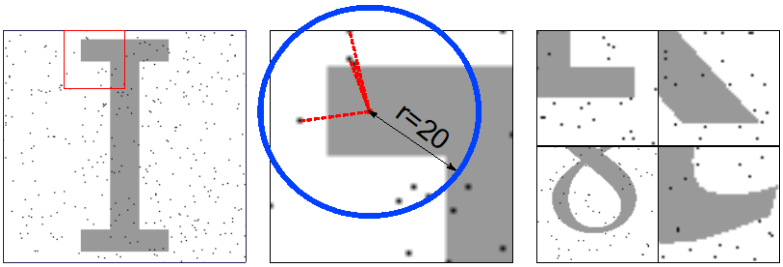

Fig. 6. Illustration of complicated situations.

The $NN(n)$ method selects n nearest neighbors from the training sample. According to this method, various amounts of different class training sample elements can be selected. There can be a situation when all selected neighbors are from the same class, therefore the classified pixel is also assigned to this class.

The $NN_C(n, m_c)$ method selects n nearest neighbors from the training sample as the $NN(n)$ method. If n_i (selected neighboring points from the i-th class) is smaller than m_c, then additional $m_c - n_i$ neighbors are selected from the training sample from the i-th class and it is done for all classes. In this case there are always at least m_c elements from all classes and this means that the information from all classes is used for classification for every pixel to be classified.

The $NN_{R1}(r_t, n)$ method selects neighbors form the training sample where the Euclidean distance between training sample pixels and pixel to be classified is smaller or equal to the radius r_t. In this case the situation can occur when no training sample is selected. Therefore, if the number of selected neighbors from the training sample is smaller than n, the radius r_t is increased until at least n neighbors are selected. Using this method the same situation as with the $NN(n)$ method can occur when all selected neighbors are from the same class, therefore another modification is needed.

The $NN_{R2}(r_t, n, m_c)$ method selects neighbors from the training sample in the same way as the $NN_{R1}(r_t, n)$ method. When at least n neighbors are selected, the radius r_t is increased until m_c training sample elements are selected for all classes.

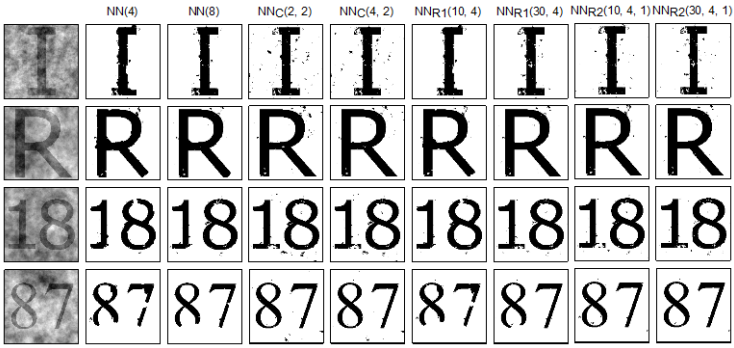

Fig. 7. Visual results of the classification. Most interesting images are presented.

In order to determine the influence of neighborhood schemes a large experiment was performed. Visual results of most interesting and important images are presented in Fig. 7. These visual results show that the best schemes, according to average classification accuracy, in some cases do not deal with harder situations when where is no training sample in specific places. The image of Fig. 7 representing number "87" is the best example. Only the methods which use at least one element from each training sample could correctly classify the bottom of the number "8".

Neighborhood schemes, which require some training samples from every class $NN_C(n, m_c)$ and $NN_{R2}(r_t, n, m_c)$ deal better with harder situations, when in some important place training samples are missing. It may become more important when a smaller training sample is given. Such schemes can help in situations when some class areas are very thin and the training samples cannot be gained from these thin areas. These different neighborhood schemes can be used in real situations, especially classifying roads or rivers from remotely sensed images.

In this chapter a generalized version of the SCRD method is presented. This version is generalized for 3D images. Experimental results of this version show that an average classification accuracy of 91.5% was obtained. This accuracy is similar to the accuracy obtained in earlier analysis of SCRD in 2D space. The generalized SCRD version allows using this method with MRT or CT medical images.

4. EYE FUNDUS BLOOD VESSEL CLASSIFICATION

In this chapter the possibilities of using statistical decisions for eye fundus images analysis automation are investigated. Methods for analyzing eye fundus images are provided. These methods use spatial information to resolve issues related to eye image analysis. The main purpose of these methods is to calculate the ratio of the width of arteries to veins – the *AVR* parameter. This parameter is significant in the diagnosis of diseases as it can help to diagnose the condition in advance and to evaluate the course.

This chapter consists of the following parts:

- First, an analysis of the eye fundus image analysis tools is performed. Then an initial analysis method was developed. An experimental study of the application of this method is described. This study raises issues related to the methods used to automate the eye fundus analysis.
- Based on the problems raised, a method for measuring the ocular blood vessels has been developed (Stabingis, et al., 2017). A description of the method and principles of the method relevant to automation are provided. By this method, measurements are made by analyzing the information of the blood vessel and its environment. This information is derived from the spatial distance function and statistical methods are used for the analysis.
- The developed method for blood vessel measurements and its possibilities of application are presented. Vessel measurements are compared with manual measurements. Automated measurements do not differ from expert measurements with a 0.95 significance level.
- Next, a fully automated method for evaluating the *AVR* parameter is presented (Stabingis et al., 2018), focusing on vascular classification of arteries and veins. The method is designed to meet the requirements of universality and adaptability to different images.

- The importance of the developed classification method is the new features used for the blood vessel measurements and the normalization based on spatial distance between the blood vessels to be classified.
- Proposed classification method is analyzed with different databases of eye fundus images and compared with similar classification methods used for the same purpose.
- In addition, a study of the proposed method is carried out using supervised methods. The aim of this study is to demonstrate the importance of the adaptability of the methods to different types of data when modeling and application are performed with different types of images.
- At the end of the chapter, the results of the research are summarized.

4.1. Description of the proposed method

Main adaptive features of the proposed method are presented in Fig. 8. These features reduce the influence of common eye fundus image analysis issues. The proposed method is adaptive to different size images; no image down sampling is applied. No parameters need to be tuned manually for different image data sets, no different models, with different parameters are created. Image noise and uneven lightening of the image is considered while creating the algorithm. All main steps: *OD* detection, blood vessel measurements, artery and vein classification and *AVR* evaluation are done automatically.

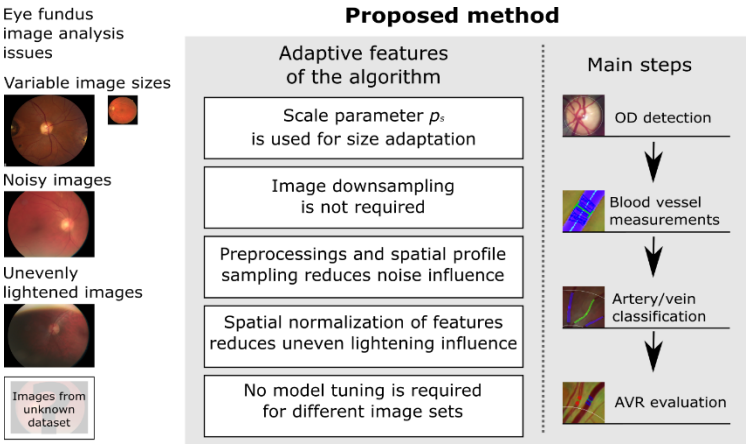

Fig. 8. Main adaptive features of the proposed method taking into account common eye fundus image analysis issues.

The main steps of an automatic algorithm for evaluation of artery and vein ratio are presented in Fig. 8. Green color channel I_G from eye fundus image is used for eye fundus mask I_M extraction. For mask extraction, common image analysis techniques are applied. After thresholding, the higher intensity part from I_G, mathematical morphology closing and flood fill operations are used to form a circular mask of eye fundus part in the image. I_M is then used to calculate the scale parameter p_s according to Eq. (13) combining a logistic growth model with a linear model.

$$p_S = \frac{\beta_1}{1+\beta_2 \cdot exp\left(-\frac{W_M}{\beta_3}\right)} + \frac{W_M}{\beta_4}, \qquad (13)$$

where β_1, β_2, β_3 are parameters of the logistic growth model part, β_4 is the parameter of the linear model part ($\beta_1 = 4$, $\beta_2 = 20$, $\beta_3 = 500$ and $\beta_4 = 3000$ in our case), W_M is the width of fundus mask I_M. Parameters are selected to form particular p_s value, which is further used in other stages as a multiplier to make other parameters adaptive. The parameter p_s evaluated by Eq. (13) is used in almost all steps of the algorithm. This parameter allows using images of different sizes.

Image pre-processing allows to unify different images and to reveal some image features required for specific operations. Image pre-

processing is treated as a vital stage for many eye fundus image analysis methods. The proposed method consists of several different large stages, and for each stage, a different image pre-processing algorithm is applied. Pre-processing allows controlling different stages separately because some methods can enhance the extraction of the blood vessel tree but reduce *OD* extraction reliability. Vessel tree I_{tr} extraction stage is not very important in the proposed algorithm because I_{tr} information is used in other stages only as auxiliary. In some other eye fundus analysis algorithms, I_{tr} extraction is very important, and the extracted tree is used as the reference for almost all other stages. Such dependence on extracted I_{tr} can lead to some errors, especially for sick patients, when some artefacts in the image can be treated as blood vessels or when vessel and background contrast is very low, producing breakage in a vessel tree. There are several different techniques for I_{tr} extraction like thresholding, mathematical morphology, Gabor filtering, wavelets etc. More precise methods are also developed. These methods produce higher extraction accuracy but require a larger amount of computations. The mathematical morphology-based method is applied here and is described in more detail in (Stabingis et al., 2018). All other stages work even without the extracted I_{tr} and in places where I_{tr} is incorrectly extracted.

4.2. Optic Nerve Disc Extraction

The *OD* extraction algorithm consists of two stages. Initial OD_{init} is located at the first stage, and then real OD_r circle is detected and evaluated. During the second stage, the circle is fitted to detect a circle like an object in the image. Full *OD* detection scheme is presented in Fig. 9.

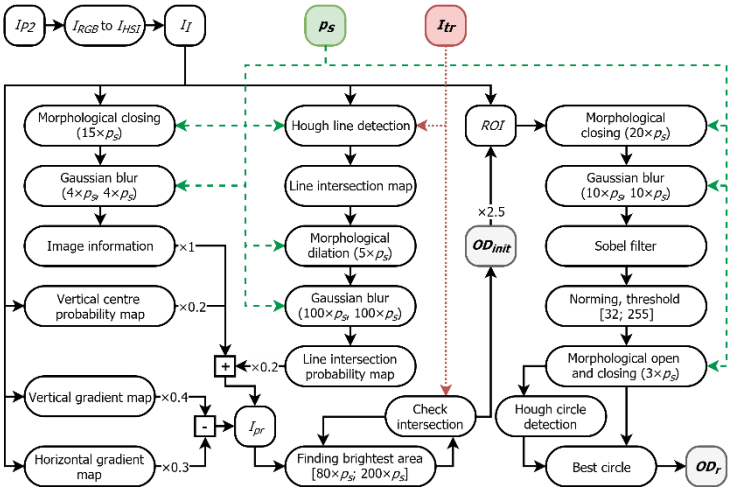

Fig. 9. Two stage OD detection scheme. Green dashed lines show the influence of scale parameter used for image size adaptation.

The first OD_{init} detection stage finds the preliminary location of *OD*. During this stage the probability map I_{pr} is created. This probability map combines the influence of five different probabilities:

- image information part I_I (coefficient 1)
- vessel tree line intersection map I_{LInt} (coefficient 0.2)
- vertical center probability map I_{VCent} (coefficient 0.2)
- vertical gradient map I_{VGr} (coefficient -0.4)
- horizontal gradient map I_{HGr} (coefficient -0.3)

I_{pr} is calculated according to Eq. (14):

$$I_{pr} = 1 \cdot I_I + 0{,}2 \cdot I_{LInt} + 0{,}2 \cdot I_{VCent} - \\ -0{,}4 \cdot I_{VGr} - 0{,}3 \cdot I_{HGr}. \qquad (14)$$

I_{pr} is used for finding the most intense circle OD_{init} with a radius from $80 \cdot p_s$ to $200 \cdot p_s$ intersecting with I_{tr}.

Normally eye fundus image is photographed in such a way that OD is located near the vertical center of the image. In order to add this feature, a vertical center probability map is calculated. To eliminate

uneven lightening vertical and horizontal gradient maps are calculated. A vertical gradient map is calculated by averaging every image row, and a horizontal gradient map is calculated by averaging every image column.

The region of interest is selected according to OD_{init} circle multiplied by 2.5, and it is used for real OD_r detection. After several image analysis and processing operations Hough circle detection is applied, and ten best circles are selected. A circle surrounded by most points from I_b is selected as OD_r and is used in further analysis.

4.3. Blood Vessel Measurements

After OD_r is detected, the information is used for vessel measurements. Measurements are made along the circle with radius $2 \cdot r_{OD}$ from OD_r center $(x_{OD}; y_{OD})$, where r_{OD} is OD_r radius. Measurements are taken at five pixel length intervals calculated according to Eq. (15).

$$\begin{cases} x_i = x_{OD} + \left(2 \cdot r_{OD} \cdot \cos(\alpha_i)\right) \\ y_i = y_{OD} + \left(2 \cdot r_{OD} \cdot \sin(\alpha_i)\right) \end{cases}, \tag{15}$$

where $\alpha_i = \alpha_{i-1} + \frac{5}{2 \cdot r_{OD}}$, $\alpha_1 = 0$ and $\alpha_i \in [0; 2\pi)$.

The method automatically detects the place where a vessel can be. After the vessel is detected and measured the algorithm goes along the detected vessel and measures other profile widths. Vessel data is collected for every vessel in the range of radiuses from $[1{,}5 \cdot r_{OD}; 3 \cdot r_{OD}]$. Average vessel width value is used for further calculations. Measurements are omitted at places where the vessel is already measured. Vessel measurements are made by analyzing vessel profile data. Profile information is gathered from the image using spatial distance based function Eq. (16). For every profile 100 intensity values are calculated from J nearest pixels.

$$v_j = \frac{\sum_{s_{i \in J}} z_i \cdot h_{ij}}{\sum_{s_{i \in J}} h_{ij}}, j = 1 \dots n_{stp}, \tag{16}$$

$$h_{ij} = \begin{cases} 1 - \frac{d(s_i, s_j)}{3}, kai\ d < 3 \\ 0, kai\ d \geq 3 \end{cases}, \quad (17)$$

where v_j is the intensity value for step j at location s_j, h_{ij} is the distance function, for $d(s_i, s_j) < 3$, $d(s_i, s_j)$ is the Euclidean distance between s_i and s_j points and z_i is intensity value at point s_i. Profile information is smoothed with Gaussian filter and analyzed for width evaluation. Profile analysis points are shown in Fig. 10.

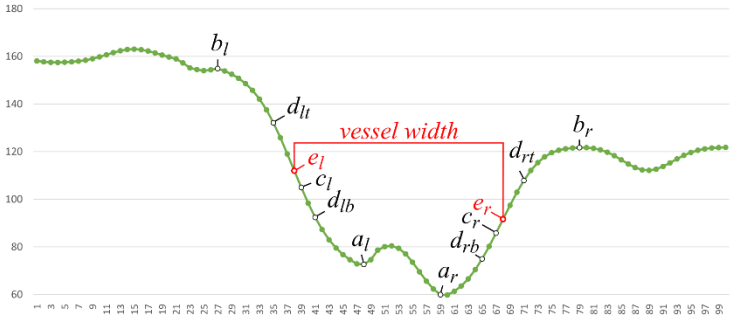

Fig. 10. Analysis of blood vessel profile.

Profile analysis steps:

- Profile minimum point is found near the profile center.
- Another close minimum point is found in order to eliminate possible central reflex information.
- Two points a_l and a_r are used as left and right profile parts.
- Local maximum points b_l and b_r are found.
- Fastest decaying points c_l and c_r are detected.
- Similarly to c_l and c_r, decaying marginal points d are selected for left and right sides.
- Middle points e_l (between d_{lb} and d_{lt}) and e_r (between d_{rb} and d_{rt}) are selected as vessel width measurement points.

Such profile analysis is performed for profiles extracted for point (x_i, y_i) at different angles and the angle with the smallest profile width is selected as profile perpendicular to a vessel. For the first measurement of the vessel, angles from 0° to 180° are analyzed, and

the detected angle is used for further vessel measurements decreasing the amount of different angles to be analyzed. Vessel measurements were compared with the measurements made by the expert and similar results were obtained.

Eighty-six images were used for evaluating the proposed algorithm and four main vessels were measured in each image: two top vessels and two bottom vessels (starting in the area of *OD*). In total, 344 measurements were made. All images were obtained by the Optomed OY digital mobile eye fundus camera Smartscope M5 PRO and, at the same places where the proposed algorithms measured vessel widths, experts measured them as well. The statistical hypothesis was tested and, with a confidence level of 95%, the expert and system measurements can be considered as the same.

4.4. Feature Extraction and Classification

Eye fundus vessel classification is a complicated task. For the proposed algorithm, novel features are extracted for classification. After analyzing many different vessels from different type images it was considered that the best part for discriminating veins from arteries is the vessel's inner part. Usually veins are darker than the arteries and arteries often have a brighter center reflex line. The outer part of different type vessels can be very similar. Three different features are extracted from vessels for classification. These features are (Fig. 10):

- an average value between a_l and a_r points
- an average value between d_{lb}, d_{rb} points
- an average value between d_{lb}, a_l , and a_r, d_{rb} points.

Features are calculated from green image channel I_G and from red channel I_R separately. These two channels are used for their best discrimination information. Average feature value is calculated along the vessel part. So, for every detected vessel, six different averaged features are calculated.

Uneven image lightening can lead to misclassification of vessels. In order to eliminate this influence, spatial distance-based normalization function Eq. (18) is applied to extracted features.

$$z_i' = \frac{z_i - \hat{\mu}_d}{\hat{\sigma}_d}, \tag{18}$$

$$\hat{\mu}_d = \sum_{i \epsilon \omega} \frac{z_i}{d_i} / \sum_{i \epsilon \omega} \frac{1}{d_i}, \tag{19}$$

$$\hat{\sigma}_d^2 = \sum_{i \epsilon \omega} \left(\frac{z_i}{d_i} - \bar{z}_d \right) / \sum_{i \epsilon \omega} \frac{1}{d_i}, \tag{20}$$

where $\hat{\mu}_d$ is the local mean and $\hat{\sigma}_d^2$ is the local variance of corresponding vessel features, ω is the set of ten closest vessels, d_i is the Euclidean distance between vessel patch centers.

After distance-based normalization, features are used for vessel classification. The *k*-means clustering method is used. Top vessels and bottom vessels according to OD_r center point are classified separately. Vessel parts used for features are brighter for arteries than for veins, so a class with a larger feature values is treated as an artery and a class with smaller feature values as vein classes. Two largest vessels from different classes are selected for the top part and for the bottom part. According to the selected vessel widths, top and bottom *AVR* values are evaluated. One eye fundus image with classification results and main analysis elements is presented in Fig. 11. The classification results and comparison are presented in the results section.

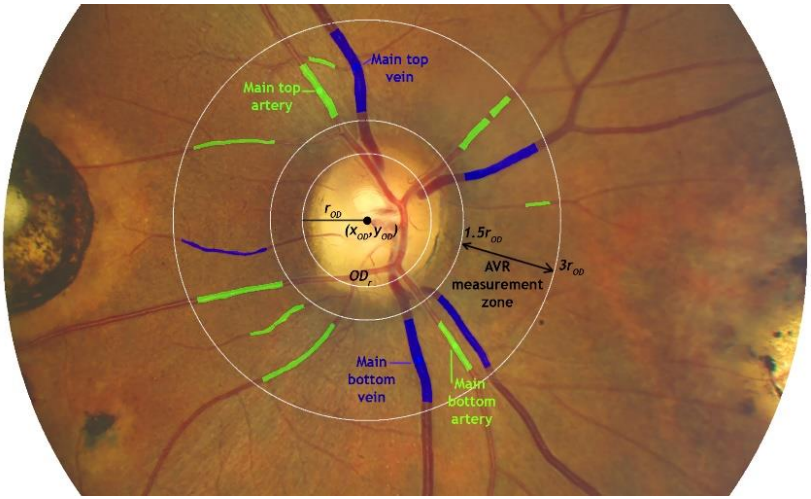

Fig. 11. Result image from *INSPIRE-AVR* database (Niemeijer et al., 2011) showing main analysis elements. Blue color – classified veins, green color – classified arteries. Main vessels used for *AVR* evaluation are marked.

4.5. Blood vessel classification results

The proposed method is tested on three eye fundus image databases. DRIVE (Staal et al., 2004) image database is one of the most popular databases for different method comparison, but this database is old, and images in this database are of small resolution – 565×584 pixels. There are 40 eye fundus images in this database. This database was selected for the comparison in order to show the method's ability to work automatically on smaller images. Another database used for comparison is INSPIRE-AVR (Niemeijer et al., 2011). There are also 40 eye fundus images in this database, and the resolution of images is 2394×2048 pixels. The method is also tested with OPTO-AVR database where images are acquired in a complicated situation involving physical exercises. Images are taken before the physical load, right after the physical load and after 45 minutes. Such an experiment is performed in order to test whether changes in *AVR* can show tiredness or stress. Photographs of both eyes are taken with Optomed OY digital mobile eye fundus camera SmartscopeM5 PRO. Image resolution is 1536 × 1152 pixels, and there are 86 images in this

database. Vessel extraction accuracy is the proportion of detected vessels. Vessels with widths larger than 3×ps and in *AVR* measurement zone are selected. Extracted vessels were classified into two classes. Classification accuracy, artery class specificity (Sp), sensitivity (Se) and area under ROC curve (AUC) statistics were calculated. The vessel detection and classification results for different databases are presented in Table 3.

Table 3. Vessel classification statistics for different databases.

Database	**Vessel extraction accuracy**	**Vessel classification statistics**			
		Accuracy	**Sp**	**Se**	**AUC**
DRIVE	0.942	0.854	0.9353	0.822	0.879
INSPIRE-AVR	0.882	0.859	0.8539	0.862	0.858
OPTO-AVR	0.904	0.835	0.8344	0.836	0.835

Methods used for vessel patch classification in *AVR* measurement zone were selected for the comparison. The selected methods are tested on INSPIRE-AVR (Niemeijer et al., 2011) and on DRIVE (Staal et al., 2004) image databases. All data used for comparison is gathered from publications that describe the methods. Performance information of these methods is presented in Table 4.

Vessel classification results compared with other methods show similar classification results. After analyzing misclassification cases, main classification errors occur due to vessel crossings and overlapping and due to lightening issues. In all images analyzed, 15 non-vessel places were recognized like vessels due to vessel-like reflections.

Table 4. Vessel classification results for similar methods.

Method	Database	Vessel classification statistics			
		Accuracy	Sp	Se	AUC
(Muramatsu et al., 2011)	DRIVE	0.928	-	0.87	-
(Mirsharifa et al., 2013)	DRIVE	0.916	-	-	-
(Dashtbozorg et al., 2014)	DRIVE	0.883	0.86	0.91	-
(Niemeijer et al., 2011)	INSIPRE-AVR	-	-	-	0.84
(Dashtbozorg et al., 2014)	INSIPRE-AVR	0.874	0.84	0.90	-

AVR evaluation was compared with publicly available INSPIRE-AVR (Niemeijer et al., 2011) data and mean absolute error MAE = 0.093 was obtained. *AVR* evaluations were compared with experts measurements performed with OPTO-AVR fundus database and MAE = 0.156 was obtained.

5. CONCLUSIONS AND RECOMMENDATIONS

1. The supervised classification method SCRD was developed, which is gaining the advantage over other similar methods because of the spatial information used in it. Method is relevant when the spatially correlated noise is in the data used for classification. Studies have shown that the method is starting to gain an advantage when the noise level is 75% of image information.
2. Experiments showed that the increase in spatial correlation width parameter α improve the classification accuracy using the proposed method. In NNet, SVM and RF methods the average accuracy is reduced by 2%, when a correlation width α increases from 10 to 20.
3. Neighbor selection methods for SCRD method were analyzed. Research showed that neighbor selection, when several points from every class is required, distinguishes the object structure from the image part when there are no training sample points in

this part. This is the case with a small training sample and when objects with thin parts are analyzed.

4. SCRD method was generalized in order to use this method for classification in 3D images. The accuracy of the classification in a 3D coordinate system is 91.5% when the noise level is 75% of image information. The extension of this method makes it possible to apply the method to medical MRI and CT images for the classification of the individual points in the case of the two classes.
5. The calculation and use of the scale parameter was proposed. This parameter helps to solve eye fundus image analysis adaptivity problems associated with changes in medical imagery.
6. The proposed method for the extraction of vessel profile information using spatial information from the image contributes to the development of the adaptive and noise-resistant blood vessels' profile analysis methods. The method is applied to the development of the measurement technique used for measuring blood vessels. Measurements coincide with those made by the expert (significance level of 0.95, $R^2 = 0.88$).
7. The classification method for blood vessels used for *AVR* parameter automatic evaluation was developed. The method was tested with three eye fundus image databases without any additional adaptation and without image resolution reduction (classification accuracy results: 0.854, 0.859 and 0.835). Proposed method uses new features and their spatial normalization, which reduces uneven lightening of the images and increases the accuracy of the classification by 6%.
8. LDA, SVM, K-NN and DT supervised classification methods were used for blood vessel classification applied for *AVR* parameter evaluation. When the same image database was used for training and for testing, the classification accuracy for some of them was higher than the accuracy of the methods used for comparison. However, when different image databases were used for the training and testing of methods, the accuracy of the classification decreased by 13% on the average.

LIST OF PUBLICATIONS ON THE TOPIC OF DISSERTATION

The results of the research were published in two peer-reviewed journals:

1. **Giedrius Stabingis**, Jolita Bernatavičienė, Gintautas Dzemyda, Alvydas Paunksnis, Lijana Stabingienė, Povilas Treigys, Ramutė Vaičaitienė, Adaptive eye fundus vessel classification for automatic artery and vein diameter ratio evaluation, *Informatica*, 2018, Vol. 29, No. 4, p. 757–771.
2. **Giedrius Stabingis**, Kęstutis Dučinskas, Lijana Stabingienė, Comparison of spatial classification rules with different conditional distributions of class label, *Nonlinear Analysis: Modeling and Control*, 2014, Volume 19, No 1, p. 109-117, MII, Vilnius. ISSN 1392-5113.

The results of the research were published in five peer-reviewed conference proceedings journals:

1. **Giedrius Stabingis**, Jolita Bernatavičienė, Gintautas Dzemyda, Alvydas Paunksnis, Povilas Treigys, Ramutė Vaičaitienė, Lijana Stabingienė, Automatization of eye fundus vessel width measurements, *VipIMAGE 2017, Lecture Notes in Computational Vision and Biomechanics*, Volume 27, pp. 787-796, 2017. Springer.
2. **Giedrius Stabingis**, Spatial classification rule with distance in three dimensional space, *Lietuvos matematikos rinkinys. Proc. of the Lithuanian Mathematical Society, Ser. A*, 2016, Vol. 57. p. 81-85, ISSN 0132-2818.
3. **Giedrius Stabingis**, Jolita Bernatavičienė, Gintautas Dzemyda, Daiva Imbrasienė, Alvydas Paunksnis, Automated Classification of Arteries and Veins in the Retinal Blood Vasculature, *Computer data analysis and modeling. Theoretical & Applied Stochastics. Proceedings 11th International Conference*, 2016, p. 64-67. Minsk, Belarus.
4. **Giedrius Stabingis**, Lijana Stabingienė, Neighborhood scheme selection for classification with SCRD method, *Lietuvos matematikos rinkinys. Proc. of the Lithuanian Mathematical Society, Ser. A*, 2015, Vol. 56, p. 101–106. ISSN 0132-2818.

5. **Giedrius Stabingis**, Lijana Stabingienė, Application of spatial classification rules for remotely sensed images, *Lietuvos matematikos rinkinys. Proc. of the Lithuanian Mathematical Society, Ser. B,* 2014, Vol. 55, p. 63–67. ISSN 0132-2818.

The results of the research were presented and discussed at eleven national and international conferences:

1. **Giedrius Stabingis**, Jolita Bernatavičienė, Gintautas Dzemyda, Alvydas Paunksnis, Povilas Treigys, Ramutė Vaičaitienė, Lijana Stabingienė. Automatic Artery Vein Ratio Measurements in Eye Fundus Images. *Data Analysis Methods for Software Systems. 9th International Workshop*. Druskininkai, Lithuania. 2017.
2. **Giedrius Stabingis**, Jolita Bernatavičienė, Gintautas Dzemyda, Alvydas Paunksnis, Povilas Treigys, Ramutė Vaičaitienė, Lijana Stabingienė, Automatization of Eye Fundus Vessel Width Measurements. *VI ECCOMAS Thematic Conference on Computational Vision and Medical Image Processing,* Porto, Portugal. 2017.
3. **Giedrius Stabingis**, Jolita Bernatavičienė, Povilas Treigys, Alvydas Paunksnis, Ramutė Vaičaitienė, Viktor Medvedev. Automated Blood Vessels Diameter Measurement in Eye Fundus Images. *Data Analysis Methods for Software Systems. 8th International Workshop*. Druskininkai, Lithuania. 2016.
4. **Giedrius Stabingis**, Jolita Bernatavičienė, Gintautas Dzemyda, Daiva Imbrasienė, Alvydas Paunksnis. Automated Classification of Arteries and Veins in the Retinal Blood Vasculature. *11th International Conference computer data analysis & modeling 2016 Theoretical & Applied Stochastics*. Minsk, Belarus. 2016.
5. Jolita Bernatavičienė, Gintautas Dzemyda, Alvydas Paunksnis, **Giedrius Stabingis**, Povilas Treigys. Automated Blood Vessel Detection and Pathological Changes Identification in Eye Fundus Images. *EURO 2016 - 28th European Conference on Operational Research*. Poznan, Poland. 2016.
6. **Giedrius Stabingis**, Spatial classification rule with distance in three dimensional space, *The 57-th conference of Lithuanian mathematical society*. Vilnius, Lithuania. 2016.
7. **Giedrius Stabingis**, Jolita Bernatavičienė, Gintautas Dzemyda, Daiva Imbrasienė, Alvydas Paunksnis, Viktorija Slavinskytė,

Povilas Treigys. Automated Blood Vessel Detection and Characteristic Evaluation in Eye Fundus Images. *Data Analysis Methods for Software Systems. 7th International Workshop*. Druskininkai, Lithuania. 2015.

8. **Giedrius Stabingis**, Lijana Stabingienė, Neighborhood scheme selection for classification with SCRD method, *The 56-th conference of Lithuanian mathematical society*. Kaunas, Lithuania. 2015.
9. **Giedrius Stabingis**, Lijana Stabingienė. The influence of noise level to the accuracy of supervised classification methods. *Data Analysis Methods for Software Systems. 6th International Workshop*. Druskininkai, Lithuania. 2014.
10. **Giedrius Stabingis**, Lijana Stabingienė, Application of spatial classification rules for remotely sensed images, *The 55-th conference of Lithuanian mathematical society*. Vilnius, Lithuania. 2014.
11. Lijana Stabingienė, **Giedrius Stabingis**. The influence of noise level to the accuracy of supervised classification methods. *1st international conference on high performance computing and mathematical modelling*. Liepaja, Latvia. 2013.

ABOUT THE AUTHOR

Giedrius Stabingis obtained BSc degree in 2005 in the field of Informatics and MCs degree in 2011 in the field of Statistics, both at Klaipėda University. He was a PhD student at Vilnius University Institute of Data Science and Digital Technologies from 2014 to 2018. Currently he is an assistant professor at the Informatics and Statistics Department of Klaipėda University. His interests include image analysis methods, image processing, classification methods, spatial statistics and spatial data mining.

LIST OF REFERENCES

1. Almotiri J., Elleithy K., Elleithy A. (2018). Retinal Vessels Segmentation Techniques and Algorithms: A Survey. *Applied Sciences*, 8(2), p. 155. doi:10.3390/app8020155
2. Atkinson P. M., Naser D. K. (2009). A geostaticilly weighted k-nn classifier for remote sensed imagery. *Geographical Analysis*, 42, p. 204–225.
3. Comber A. J. (2013). Geographically weighted methods for estimating local surfaces of overall, user and producer accuracies. *Remote Sensing Letters*, 4, p. 373–380.
4. Cressie N. (1993). *Statistics for Spatial Data revised edition.* New York: Wiley.
5. Dashtbozorg B., Mendonca A. M., Campilho A. (2014). An Automatic Graph-Based Approach for Artery/Vein Classification in Retinal Images. *IEEE Transactions on Image Processing*, 23(3), p. 1073–1083.
6. Dučinskas K. (2009). Approximation of the expected error rate in classification of the Gaussian random field observations. *Statistics and Probability Letters*, 79.
7. Fraz M. M., Rudnicka A. R., Owen C. G., Strachan D. P., Barman S. A. (2014). Automated arteriole and venule recognition in retinal images using ensemble classification. *2014 International Conference on Computer Vision Theory and Applications (VISAPP)*, 3, p. 194–202.

8. Guo L., Chen L., Chen C. P., Zhou J. (2018). Integrating guided filter into fuzzy clustering for noisy image segmentation. *Digital Signal Processing*, 83, p. 235-248. doi:10.1016/j.dsp.2018.08.022
9. Haralick R. M. (1979). Statistical and structural approaches to texture. *Proceedings of the IEEE*, 67, p. 786–804.
10. Yosinski J., Clune J., Bengio Y., Lipson H. (2014). How transferable are features in deep neural networks? *Advances in Neural Information Processing Systems*, 27, p. 3320–3328.
11. Ji S., Xu W., Yang M., Yu K. (2013). 3D Convolutional Neural Networks for Human Action Recognition. *IEEE Transactions on Pattern Analysis and Machine Intelligence*, 35(1), p. 221–231. doi:10.1109/TPAMI.2012.59
12. Krishnan S., Athavale Y. (2018). Trends in biomedical signal feature extraction. *Biomedical Signal Processing and Control*, 43, p. 41–63. doi:10.1016/j.bspc.2018.02.008
13. Krizhevsky A., Sutskever I., Hinton G. E. (2012). ImageNet Classification with Deep Convolutional Neural Networks. *Proceedings of the 25th International Conference on Neural Information Processing Systems*, 1, p. 1097–1105.
14. LeCun Y., Bengio Y., Hinton G. (2015). Deep learning. *Nature, 521*, p. 436–444. doi:10.1038/nature14539
15. Li M., Zang S., Zhang B., Li S., Wu C. (2014). A Review of Remote Sensing Image Classification Techniques: the Role of Spatio-contextual Information. *European Journal of Remote Sensing*, 47, p. 389–411.
16. Li X., Wee W. G. (2014). Retinal vessel detection and measurement for computer-aided medical diagnosis. *Journal of Digital Imaging*, 27(1), p. 120–132.
17. Liu J. G., Mason P. J. (2009). *Essential image processing and GIS for remote sensing.* UK: Wiley-Blackwell.
18. Miri M., Amini Z., Rabbani H., Kafieh R. (2017). A Comprehensive Study of Retinal Vessel Classification Methods in Fundus Images. *Journal of Medical Signals & Sensors*, 7(2), p. 59–70.

19. Mirsharifa Q., Tajeripoura F., Pourreza H. (2013). Automated characterization of blood vessels as arteries and veins in retinal images. *Computerized Medical Imaging and Graphics*, 37, p. 607–617.
20. Mun J., Jang Y., Nam Y., Kim J. (2018). Edge-enhancing bi-histogram equalisation using guided image filter. *Journal of Visual Communication and Image Representation*. doi:10.1016/j.jvcir.2018.12.037
21. Muramatsu C., Hatanaka Y., Iwase T., Hara T., Fujita H. (2011). Automated selection of major arteries and veins for measurement of arteriolar-to-venular diameter ratio on retinal fundus images. *Computerized Medical Imaging and Graphics*, 35, p. 472–480.
22. Neverova N., Wolf C., Taylor G. W., Nebout F. (2016). ModDrop: adaptive multi-modal gesture recognition. *IEEE Transactions on Pattern Analysis and Machine Intelligence*, 38(8), p. 1692–1706.
23. Niemeijer M., Gupta P., Ginneken B. V., Folk J., Abramoff M. (2011). Automated Measurement of the Arteriolar-To-Venular Width Ratio in Digital Color Fundus Photographs. *IEEE Transactions on Medical Imaging*, 30(11), p. 1941–1950.
24. Öztürk Ş., Akdemir B. (2018). Application of Feature Extraction and Classification Methods for Histopathological Image using GLCM, LBP, LBGLCM, GLRLM and SFTA. *Procedia Computer Science*, 132, p. 40–46. doi:10.1016/j.procs.2018.05.057
25. Sim D. A., Keane P. A., Tufail A., Egan C. A., Aiello L. P., Silva P. S. (2015). Automated retinal image analysis for diabetic retinopathy in telemedicine. *Current Diabetes Reports 15:14*. doi:10.1007/s11892-015-0577-6
26. Staal J., Abramoff M., Niemeijer M., Viergever M. A., Ginneken B.V. (2004). Ridge based vessel segmentation in color images of the retina. *IEEE Transactions on Medical Imaging*, 23, p. 501–509.
27. Stabingienė L. (2012). *Vaizdų analizė naudojant Bajeso diskriminantines funkcijas.* Vilnius: Vilnius University.
28. Switzer P. (1980). Extensions of linear discriminant analysis for statistical classification of remotely sensed satellite imagery. *Mathematics in Geology*, 12(4), p. 367–376.

29. Taigman Y., Yang M., Ranzato M., Wolf L. (2014). DeepFace: Closing the Gap to Human-Level Performance in Face Verification. *2014 IEEE Conference on Computer Vision and Pattern Recognition*, p. 1701–1708. doi:10.1109/CVPR.2014.220
30. Troya-Galvis A., Gançarski P., Berti-Équille L. (2018). Remote sensing image analysis by aggregation of segmentation-classification collaborative agents. *Pattern Recognition*, 73, p. 259–274. doi:10.1016/j.patcog.2017.08.030
31. Wang L., Shi C., Diao C., Ji W., Yin D. (2016). A survey of methods incorporating spatial information in image classification and spectral unmixing. *International Journal of Remote Sensing*, 37(16), p. 3870–3910. doi:10.1080/01431161.2016.1204032

STATISTINIAI SPRENDIMAI ERDVINEI INFORMACIJAI SKAITMENINIUOSE VAIZDUOSE

1. Tyrimų sritis

Pagrindinis vaizdų analizės tikslas – iš vaizduose esančios informacijos gauti tiriamai sričiai reikalingų žinių, kurios paskui naudojamos sprendimams priimti. Erdvinė informacija nusako ryšį tarp erdvinių duomenų ir šių duomenų požymius. Vaizdų analizėje objektais, kuriems būdinga erdvinė informacija, yra laikomi visi vaizdai, tam tikros vaizde ar vaizdų rinkiniuose esančios sritys ir atskiri vaizdo taškai. Šiame darbe yra nagrinėjamas erdvinės informacijos naudojimas vaizduose ir jų rinkiniuose (vaizduose su trimatėmis erdvinėmis koordinatėmis) esantiems objektams – atskiriems taškams ir taškų rinkiniams – tirti. Tokią objektų visumą nusako ne tik padėtis erdvėje, bet ir jų tarpusavio ryšiai: erdvinis atstumas, erdvinė priklausomybė – erdvinė autokoreliacija, klasių žymių informacija ir kita su objektais susieta statistinė informacija. Taip pat nagrinėjamos ir vaizduose esančių objektų erdvinės informacijos naudojimo kitai informacijai gauti galimybės, t. y. vaizdo dydžio ar jame esančio pagrindinio objekto dydžio naudojimas analizės metodų universalumui gauti.

2. Darbo aktualumas

Duomenų rinkimas skaitmeninių vaizdų pavidalu yra neatsiejamas nuo daugelio šiandieninio gyvenimo sričių. Vaizdai renkami ir archyvuojami beveik visose srityse. Dėl vaizdų gavimo techninės įrangos pažangos vaizdų gavimas, kaupimas ir analizė tampa neatsiejama biomedicinos, inžinerijos, gamtos bei socialinių mokslų dalimi. Vaizdų analizė jau yra svarbus informacijos gavimo įrankis, o tobulėjant vaizdų gavimo įrangai atsiranda naujų iššūkių ir galimybių.

Erdvinės informacijos naudojimo vaizdų klasifikavimui galimybės tyrinėjamos jau seniai (Haralick, 1979), o tobulėjant techninėms duomenų analizės galimybėms šių tyrimų aktualumas tik didėja (Wang et al., 2016). Vaizdų analizės ir apdorojimo praktikoje yra naudojama labai daug įvairių metodų, sukurtų seniai ir tinkamų daugeliui problemų spręsti. Tačiau šie metodai tyrinėjami ir

tobulinami dar ir šiandien (žr. Wang et al., 2016; Miri et al., 2017; Troya-Galvis et al., 2018). Daug dėmesio skiriama vaizdų filtravimo (žr. Mun et al., 2018; Guo et al., 2018), objektų išskyrimo, segmentavimo, atpažinimo, klasifikavimo (žr. Öztürk et al., 2018; Krishnan et al., 2018) ir kitiems metodams.

Vienas iš vaizdų klasifikavimo keblumų yra stebimo vaizdo suskirstymas į keletą atskirų regionų sužymint vaizdo taškus. Tai atliekama atsižvelgiant į taškų požymius ir į informaciją apie erdvinius sąryšius su mokymo imtimi. P. Switzeris buvo pirmasis, pritaikęs erdvinės informacijos sąryšius klasifikavimui (Switzer, 1980). Vaizdų klasifikavimui plačiai taikomi geostatistiniai metodai. Šie metodai remiasi erdvine autokoreliacija, ja nurodomas laipsnis, kuriuo koreliacija keičiasi kintant atstumui tarp objektų (Liu et al., 2009), ir ji tyrinėjama daugelio autorių siūlomuose metoduose (žr. Atkinson et al., 2009; Comber, 2013; Li et al., 2014). Erdvinė autokoreliacija taikoma Bajeso diskriminantinėse funkcijose, kai vertinami parametrai laikomi nekoreliuojantys su mokymo imties objektais. Straipsnyje (Dučinskas, 2009) įvestas parametrų vertinamas atsižvelgiant į erdvinę priklausomybę su mokymo imtimi. Bajeso diskriminantinių funkcijų taikymas vaizdų analizėje ir erdvinės koreliacijos įtaka nagrinėtos disertacijoje (Stabingienė, 2012).

Akies dugno kraujagyslės yra vienintelės žmogaus kraujagyslės, kurios gali būti stebimos neinvaziniu vaizdų gavimo būdu (Miri et al., 2017), (Fraz et al., 2014). Akies dugno vaizdams yra dažnai taikoma rankinė ir automatinė struktūros analizės (Mirsharifa et al., 2013), (Sim et al., 2015). Ši analizė padeda lengviau diagnozuoti ligas, tad ypač tai aktualu ankstyvosiose ligos stadijose (Li et al., 2014). Daugybė ligų gali būti iš anksto diagnozuotos iš akies dugno vaizdų remiantis keletu skirtingų požymių. Oftalmologai sieja tam tikrus arterijų ir venų pločių požymius su tokiomis ligomis, kaip diabeto retinopatija, aterosklerozė, hipertenzija ir kt. Ligos paveikia arterijas ir venas, tad susiformuoja neįprastas jų pločių santykis.

Pastaruoju metu, kai atsirado daugiau techninių galimybių, pradėti tyrinėti ir taikyti giliojo mokymosi (angl. *Deep Learning*) metodai (LeCun et al., 2015). Vaizdų analizėje pradėti plačiai taikyti konvoliuciniai neuroniniai tinklai (Krizhevsky et al., 2012), padedantys išspręsti labai sudėtingas problemas. 3D konvoliucinis neuroninis tinklas taikomas žmogaus veiksmams atpažinti iš vaizdo

medžiagos (Ji et al., 2013). Adaptyvi gestų atpažinimo sistema publikuota straipsnyje (Neverova et al., 2016). Žmogaus veido analizės galimybės „DeepFace“ sistemoje pateiktos straipsnyje (Taigman et al., 2014). Taip pat tiriamos ir pačių metodų galimybės (Yosinski et al., 2014). Ne išimtis tapo ir akies dugno vaizdų analizė, čia ji taikoma įvairiose srityse (Almotiri et al., 2018). Konvoliuciniuose neuroniniuose tinkluose naudojama iš skaitmeninių vaizdų gauta informacija apie juose esančius objektus įvairiais vaizdų apdorojimui plačiau taikomais filtrais. Taip pat informacijos trūkumo problemos sprendžiamos vaizdų augmentacija, kurioje taip pat taikomi įvairūs vaizdų analizės metodai. Šie pavyzdžiai iliustruoja tai, kad žinios apie skaitmeniniuose vaizduose esančius dėsningumus gali būti panaudotos ir tobulinant esamus ar kuriant naujus tiek giliojo mokymosi, tiek ir kitus ateityje tapsiančius aktualius metodus.

3. Darbo tikslas ir uždaviniai

Darbo tikslas – atrasti naujų statistinių sprendinių erdvinei informacijai skaitmeniniuose vaizduose pritaikyti ir ištirti taikymo galimybes akies dugno vaizdams analizuoti.
Darbo objektas – erdvinė informacija skaitmeniniuose vaizduose.
Tikslui pasiekti sprendžiami uždaviniai:

1. Išanalizuoti erdvinės koreliacijos įtaką klasifikavimo su mokymu metodams.
2. Įvesti erdvinės koreliacijos įtaką į apriorinių klasės žymių statistinį tikimybių vertinimą Bajeso diskriminantinėse funkcijose.
3. Pasiūlyti naujus kaimynystės aprašymo būdus ir ištirti jų įtaką klasifikavimui. Rasti geriausią kaimynystės aprašymo būdą nuo mokymo imties nutolusių vaizdo vietų klasifikavimui.
4. Išanalizuoti akių dugno statistinius vaizdų analizės metodus, taikomus akies dugno kraujagyslių tyrimams.
5. Rasti erdvinės informacijos pritaikymo galimus statistinius sprendimus akies dugno kraujagyslių matavimams.
6. Pritaikyti erdvinę informaciją akies dugno kraujagyslių klasifikavimo problemoms spręsti.

4. Mokslinis naujumas

1. Sukurtas klasifikavimo metodas SCRD, kuriame klasių apriorinės tikimybės priklauso nuo mokymo imties atsižvelgiant į erdvinę koreliaciją.
2. Išanalizuota kaimynų parinkimo būdų įtaka klasifikavimo su mokymu tikslumui ir nustatytas tinkamiausias iš būdų SCRD metodui.
3. Erdviniu atstumu ir koreliacija paremtas klasifikavimo metodas SCRD apibendrintas duomenims su trimatėmis erdvinėmis koordinatėmis.
4. Sukurtas adaptyvus akies dugno vaizdų analizės metodas.
5. Erdvinio atstumo funkcija pritaikyta vaizdo profilio informacijai gauti ir taikoma kraujagyslių matavimams akies dugno vaizduose.
6. Sukurtas automatinis akies dugno kraujagyslių, naudojamų arterijų ir venų santykio skaičiavimams, klasifikavimo metodas paremtas požymių erdviniu normalizavimu.

5. Ginamieji teiginiai

1. Apriorinės klasių žymių tikimybės priklauso nuo klasifikuojamo taško aplinkoje esančios mokymo imties elementų erdvinės koreliacijos.
2. Klasifikuojamo taško kaimynų parinkimo būdo pasirinkimas padeda tiksliau klasifikuoti vaizdų vietas, kurių aplinkoje trūksta vienos klasės mokymo imties elementų.
3. Erdvinių funkcijų taikymas vaizdo profilio informacijai gauti įgalina adaptyviai taikyti bendrą matavimo metodą skirtingų dydžių akies dugno vaizdams.
4. Erdvinis atstumas, taikomas klasifikavimui naudojamiems požymiams normalizuoti, padeda sumažinti netolygaus vaizdo apšvietimo sukeliamus netikslumus.

6. Darbo rezultatų aprobavimas

Tyrimų rezultatai publikuoti 2-uose periodiniuose recenzuojamuose leidiniuose, 5-iuose recenzuojamuose konferencijos pranešimų medžiagos leidiniuose, pristatyti ir aptarti 11-oje nacionalinių ir tarptautinių konferencijų.

7. Disertacijos struktūra

Disertaciją sudaro 5 skyriai ir literatūros sąrašas. Disertacijos skyriai: įvadas, erdvinė informacija ir vaizdų analizė, erdvinė klasifikavimo taisyklė, akies dugno kraujagyslių klasifikavimas ir išvados. Disertacijoje pateikti paveikslų, lentelių, naudotų santrumpų ir žymėjimų sąrašai. Visa disertacijos apimtis yra 110 puslapių, pateikti 36 paveikslai ir 10 lentelių. Disertacijoje remtasi 125 literatūros šaltiniais.

8. Išvados ir rekomendacijos

1. Sukurtas klasifikavimo su mokymu SCRD metodas, kuris tampa pranašesnis už kitus panašius metodus dėl naudotos erdvinės informacijos. Pateiktas metodas naudojamas tada, kai klasifikuojamuose duomenyse yra erdvėje koreliuoto triukšmo. Triukšmo tyrimais nustatyta, kad metodas tampa pranašesnis nuo tada, kai triukšmas sudaro 75 % vaizdo informacijos.
2. Atlikus eksperimentus nustatyta, kad pasiūlyto metodo klasifikavimo tikslumas didėja, kai didėja erdvinės koreliacijos plotis α. Tuo tarpu įprastų klasifikavimo metodų (NNet, SVM, RF) tikslumas mažėja (kai α parametras padidėja nuo 10 iki 20, tikslumas sumažėjo 2 %).
3. Ištyrus kaimynų parinkimo būdus SCRD metodui, nustatyta, kad kai imama po keletą mokymo imties taškų iš kiekvienos klasės, tiksliau išskiriama vaizde esančio objekto struktūra, kai tam tikrose to objekto dalyse nėra mokymo imties taškų. Tai aktualu turint mažą mokymo imtį ir kai reikia išskirti plona struktūra pasižyminčius objektus.

4. SCRD metodo apibendrinimas sudaro galimybes naudoti metodą 3D vaizdams klasifikuoti. Klasifikavimo tikslumas trimatėje koordinačių sistemoje siekia 91,5 %, kai triukšmas sudaro 75 % vaizdo informacijos. Šis išplėtotas metodas sudaro galimybes taikyti metodą medicininių MRT ir KT vaizdų atskiriems taškams klasifikuoti dviejų klasių atveju.
5. Darbe pasiūlytas skalės parametro apskaičiavimo ir taikymo būdas, kuris padeda spręsti akies dugno vaizdų analizės automatizavimo problemas susijusias su kintančia medicininių vaizdų raiška.
6. Pasiūlytas vaizdo profilio informacijos išskyrimo metodas, kuris padeda kurti adaptyvius ir lokaliam triukšmui atsparius kraujagyslių analizės metodus. Metodas pritaikytas akies dugno kraujagyslių matavimams, kurie sutampa su ekspertų matavimais (su 0,95 reikšmingumo lygmeniu, $R^2 = 0{,}88$).
7. Sukurtas automatinis *AVR* matavimams skirtų kraujagyslių klasifikavimo metodas. Metodas testuotas su trimis akies dugno vaizdų bazėmis be papildomos kiekvienos iš jų adaptacijos ir nekeičiant vaizdų raiškos (klasifikavimo tikslumo įverčiai: 0,854, 0,859 ir 0,835). Metode naudojami nauji pasiūlyti požymiai ir jų erdvinis normalizavimas, kuris sumažina netolygaus apšvietimo įtaką ir klasifikavimo tikslumą padidina vidutiniškai 6 %.
8. *AVR* matavimams skirtų kraujagyslių klasifikavime pritaikyti klasifikavimo su mokymu metodai (LDA, SVM, K-NN ir DT). Kai jų mokymui ir testavimui naudojama ta pati vaizdų bazė, kai kurių metodų klasifikavimo tikslumas viršija lyginimui naudotų metodų tikslumą. Tačiau kai metodų mokymui ir testavimui naudojamos skirtingos vaizdų bazės, klasifikavimo tikslumas vidutiniškai sumažėja 13 %.

TRUMPAI APIE AUTORIŲ

Giedrius Stabingis Klaipėdos universitete įgijo informatikos bakalauro (2005 m.) ir statistikos magistro (2011 m.) laipsnius. 2014–2018 m. studijavo informatikos krypties doktorantūrą Vilniaus universiteto Duomenų mokslo ir skaitmeninių technologijų institute. Nuo 2011 m. dirba Klaipėdos universitete, informatikos ir statistikos katedroje. Moksliniai interesai: vaizdų analizės metodai, vaizdų apdorojimas, klasifikavimo metodai, erdvinė statistika ir erdvinė duomenų gavyba.

Giedrius Stabingis

STATISTICAL DECISIONS FOR SPATIAL INFORMATION IN DIGITAL IMAGES

Summary of a Doctoral Dissertation
Natural Sciences
Informatics (N 009)
Editor Zuzana Šiušaitė

Giedrius Stabingis

STATISTINIAI SPRENDIMAI ERDVINEI INFORMACIJAI SKAITMENINIUOSE VAIZDUOSE

Daktaro disertacijos santrauka
Gamtos mokslai
Informatika (N 009)
Redaktorė Jorūnė Rimeisytė – Nekrašienė

Vilniaus universiteto leidykla
Saulėtekio al. 9, LT-10222 Vilnius
El. p. info@leidykla.vu.lt,
www.leidykla.vu.lt
Tiražas 50 egz.